



Synthesis, Antimicrobial Activity and Molecular Docking of Novel Series of Phthalazine Derivatives



Marwa M. Rezk^{*a}, A.A.F. Wasfy^a, Mohamed S. Behalo^a, Samar El-Kalyoubi^b, Aly A. Aly^a

^a Chemistry Department, Faculty of Science, Benha University, Benha, P.O Box 13518, Egypt

^b Pharmaceutical Organic Chemistry, Faculty of pharmacy, Port Said University, Port Said, P.O Box 42511, Egypt

Abstract

A straightforward and effective method for synthesizing phthalazine derivatives was developed through the reaction of 1-(4-(4-chlorophthalazin-1-yl)phenyl)-pyrrolidine-2,5-dione (**3**), a key precursor, with various nucleophiles containing carbon, nitrogen, oxygen, and sulfur. The structures of all synthesized compounds were verified through elemental analysis and spectral data. Furthermore, certain derivatives were assessed for their antibacterial and antifungal activities and compared with standard drugs. Among them, compounds **4**, **14a**, **15**, and **18** demonstrated antimicrobial activity, positioning them as promising candidates for therapeutic use. In vitro testing demonstrated their potent efficacy against bacterial strains (*Escherichia Coli*, *Staphylococcus Aureus*) and fungal pathogens (*Aspergillus niger*), indicating broad-spectrum antimicrobial potential. Molecular docking analyses supported these findings, revealing strong binding interactions with key microbial enzymes, which aligns with their observed inhibitory effects. Combining potent antimicrobial activity and favorable pharmacokinetic characteristics, these compounds emerge as promising leads for the development of multitarget drugs targeting infectious diseases.

Keywords: Phthalazin-1-(2H)-one, Chlorophthalazine, Pyrrolidine-2,5-dione, Antimicrobial activity, Molecular docking

Introduction

Biologically essential molecules, such as DNA, RNA, and vitamins, frequently contain heterocyclic core rings. These structural motifs play a fundamental role in numerous biochemical and physiological processes, making them indispensable to life. Their unique electronic and steric properties contribute to crucial biological functions, including enzymatic regulation, signal transduction, and genetic information storage.

The significance of heterocyclic systems has driven advancements in medicinal chemistry, particularly in the synthesis of novel therapeutic agents [1-5].

Among these, Phthalazines, a class of nitrogen-containing heterocycles, have attracted significant attention for their wide-ranging pharmacological activities, particularly in cancer drug development [6]. Among them, 4-substituted phthalazine derivatives have shown diverse therapeutic potential, such as anti-inflammatory [7-8], antimicrobial [9-14], antitumor agents [15-18], anticonvulsant, and vasorelaxant effects [19-20]. Moreover, phthalazine-based scaffolds are antimalarial applications in commercially available pharmaceuticals, including aminophthalazine and hydrazinylphthalazine derivatives found in drugs such as hydralazine [21] and carbazeran [22] both utilized in heart failure management, as well as in potent anticancer agents [23].

The phthalazine derivative azelastine also functions as an antihistamine, widely used for treating allergic rhinitis [24]. In recent years, increasing interest in targeted cancer therapies has led to the development of VEGFR-2 inhibitors, including

*Corresponding author e-mail: Marwa_3336@yahoo.com.; (Marwa Mohamed Rezk).

Received date 13 March 2025; Revised date 10 April 2025; Accepted date 13 May 2025

DOI: 10.21608/EJCHEM.2025.361774.11447

©2025 National Information and Documentation Center (NIDOC)

phthalazinone derivatives such as vatalanib and ZD 6474, which have shown promise in inhibiting angiogenesis and tumor progression[25-26] (Figure 1).

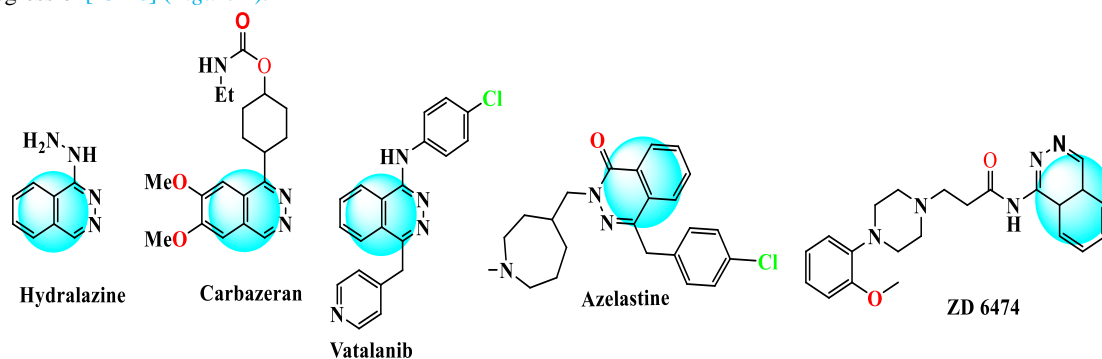


Figure 1: Various structures of biologically active phthalazine derivatives

Additionally, the phthalazine ring has demonstrated efficacy as a robust scaffold in designing melatonin MT1 and MT2 ligands, acting as bioisosteric analogs of agomelatine, a compound known for its role in regulating circadian rhythms and antidepressant activity[27]. Despite significant progress in antimicrobial drug development, the continuous emergence of resistant microorganisms remains a critical challenge, highlighting the need for novel and more potent therapeutic agents[28-35]. In response, medicinal chemists have focused on designing small molecules capable of overcoming resistance mechanisms. Phthalazine derivatives, with their diverse structural modifications, have shown promise in this regard, displaying activity against Gram-positive and Gram-negative bacteria, fungi, and even mycobacterial infections. In this context, molecular docking has become an essential computational tool for predicting the interactions between small molecules and protein targets, offering valuable visions into binding affinity and biological activity, which are crucial for rational drug design. Advances in docking algorithms have further refined the accuracy of interaction predictions, facilitating the identification and optimization of promising drug candidates[36]. These studies help assess binding interactions and potential biological effects, thereby establishing a foundation for evaluating the therapeutic relevance of newly synthesized compounds.[37-39]. Building upon these insights, our study focuses on the synthesis of novel phthalazine derivatives incorporating a pyrrolidine-2,5-dione moiety, a pharmacophore known for its significant bioactivity in antimicrobial and anticancer agents. By integrating this moiety into the phthalazine core, we aim to enhance the biological profile of these derivatives. Furthermore, we conducted molecular docking studies to investigate their potential interactions with key microbial and enzymatic targets, thereby evaluating their pharmaceutical potential.

2. Materials and Methods

2.1 Materials

All chemical reagents utilized in this study were sourced from Sigma-Aldrich, while analytical-grade solvents were procured from El-Nasr Chemicals company. The melting points of the synthesized compounds were determined using a Gallen-Kamp melting point apparatus, with all reported values remaining uncorrected. For spectroscopic characterization, infrared (IR) spectra were recorded using potassium bromide (KBr) pellets on a ThermoFisher Nicolet iS10 FT-IR spectrometer. Nuclear Magnetic Resonance (NMR) spectroscopy was performed in dimethyl sulfoxide (DMSO- d_6) as the solvent. ^1H NMR spectra were recorded at 400 MHz and ^{13}C NMR spectra at 100 MHz using a Bruker NMR spectrometer. Additionally, high-resolution ^1H and ^{13}C NMR spectra were acquired at 500 MHz on a Jeol Resonance spectrometer, with tetramethylsilane (TMS) serving as the internal reference. All chemical shifts were reported in delta (δ) values, expressed in parts per million (ppm). For mass spectrometric analysis, data were obtained via direct inlet injection, interfaced with a Thermo Scientific GC/MS model ISQ. The antimicrobial activity of the synthesized compounds was evaluated at the Micro Analytical Center, Cairo University.

2.2 Synthesis

4-(4-Aminophenyl)phthalazin-1(2H)-one (1)

A suspension of 4-(4-amino-benzoyl)-benzoic acid (10 mmol) in absolute ethanol (15 mL) was prepared, and subsequently, hydrazine hydrate (240 mmol) was added. The reaction mixture was subsequently subjected to reflux heating for a period of six hours [15-16]. The reaction mixture was cooled and filtered, resulting in the precipitation of a solid, recrystallized from a DMF/ H_2O mixture to afford compound **1** as brown crystals. Yield 50%. M.p 250–252°C. IR (KBr, cm^{-1}): 3400, 3254, 3156, 3100 (NH_2 , $\text{NH}\sim\text{OH}$), 1666 ($\text{C}=\text{O}$). ^1H NMR (DMSO- d_6 , 500 MHz, δ , ppm): 7.24–7.57 (m, 8H, aromatic protons), 9.96 (s, 2H, NH_2), 13.15 (s, 1H, $\text{NH}\sim\text{OH}$, exchangeable with D_2O). ^{13}C NMR (DMSO- d_6 , 400 MHz, δ , ppm): 168.28, 167.01, 133.02, 131.91, 131.54, 130.71, 129.37, 129.02, 128.85, 128.62, 128.06, 127.41, 123.42, 122.93. MS, m/z = 237 (M^+ , 21.44%), Anal. calcd for $\text{C}_{14}\text{H}_{11}\text{N}_3\text{O}$ (237.26). C, 70.87%; H, 4.67%; N, 17.71%; Found: C, 70.85 %; H, 4.69 %; N, 17.70%.

1-(4-(4-Oxo-3,4-dihydrophthalazin-1-yl)phenyl)pyrrolidine-2,5-dione (2)

An equimolar mixture of **1** (10 mmol), fused with succinic anhydride (10 mmol) at 250°C for 2hrs. After cooling, the precipitated triturated with H₂O and the resultant mixture obtained filtered off and recrystallized from ethanol to give **2** as pale yellow crystals. Yield 90%. M.p 203–205°C. IR (KBr, cm⁻¹) : 3467 - 3158 (NH, OH), 1780 - 1700 (C=O), 1590 (C=N). ¹H NMR (DMSO-d₆, 500 MHz, δ, ppm) : 2.02 (m, 4H, 2CH₂), 6.98–7.56 (m, 8H, aromatic protons), 9.92 (s, 1H, NH, exchangeable), 12.88 (s, 1H, OH, exchangeable). ¹³C NMR (DMSO-d₆, 100 MHz, δ, ppm) : 167.5 (CO_{imide}), 159.58 (CO), 137.57, 135.18, 135.02, 133.52, 132.38, 132.01, 129.32, 128.82, 128.54, 127.88, 126.99, 125.99, 123.89 (aromatic carbons), 29.26. Ms, m/z = 319 (M⁺, 36.26%). Anal. calcd for C₁₈H₁₃N₃O₃ (319.93). C, 67.71%; H, 4.10%; N, 13.16%; O, 15.03%; Found C, 67.65%; H, 3.99%; N, 13.20%; O, 15.15%.

1-(4-(4-Chlorophthalazin-1-yl)phenyl)pyrrolidine-2,5-dione (3)

A mixture of phosphorus pentachloride (10 mmol), phosphorus oxychloride (20 mmol), and phthalazinone **2** (10 mmol) was heated under reflux in a water bath for 4 hours. then reaction mixture was cooled and poured onto crushed ice. The resulting solid was collected by filtration, thoroughly washed with water, dried, and recrystallized from ethanol, yielding compound **3** as off-white crystals. Yield 80%. M.p 233–235°C. IR (KBr, cm⁻¹) : 3020 (CH aromatic), 1744 - 1662 (C=O), 1555 (C=N), 709 (C-Cl). ¹H NMR (DMSO-d₆, 500 MHz, δ, ppm) : 2.02 (m, 4H, 2CH₂), 7.28–7.94 (m, 8H, aromatic protons). ¹³C NMR (DMSO-d₆, 100 MHz, δ, ppm) : 167.48 (CO_{imide}), 159.58 (C-Cl), 150.58, 135.02, 132.38, 132.01, 129.32, 128.82, 128.54, 125.99, 123.80, 123.89 (aromatic carbons), 29.26. Ms, m/z = 337 (M⁺, 14.66%), 338 (M+1, 17.64%). Anal. calcd for C₁₈H₁₂ClN₃O₂ (337.76). C, 64.01%; H, 3.58%; Cl, 10.50%; N, 12.44%; O, 9.47%. Found C, 63.98%; H, 3.50%; Cl, 10.55%; N, 12.49%; O, 9.40%.

1-(4-(4-Methoxyphthalazin-1-yl)phenyl)pyrrolidine-2,5-dione (4)

A solution of compound **3** (10 mmol) and sodium methoxide (10 mmol) in methanol (30 mL) was refluxed for 6 hours. After cooling, the reaction mixture was poured into an ice/HCl solution. The resulting precipitate was collected by filtration and recrystallized from ethanol, yielding compound **4** as pale brown crystals. Yield 60%. M.p 170–172°C. IR (KBr, cm⁻¹) : 2920 - 2868 (CH aliphatic), 1778 - 1707 (C=O), 1383 (-OCH₃), 1575 (C=N). ¹H NMR (DMSO-d₆, 500 MHz, δ, ppm) : 2.09 (m, 4H, 2CH₂), 4.45 (s, 3H, CH₃), 7.90–8.04 (m, 8H, aromatic protons). ¹³C NMR (DMSO-d₆, 500 MHz, δ, ppm) : 170.08 (C-O-C), 167.07 (CO_{imide}), 159.13, 134.75, 134.61, 133.11, 131.92, 131.58, 128.89, 128.37, 128.11, 127.48, 126.55, 125.58, 123.46 (aromatic carbons), 54.50, 30.0 (aliphatic carbons). Ms, m/z = 333 (M⁺, 29.98%). Anal. calcd for C₁₉H₁₅N₃O₃ (333.35). C, 68.46%; H, 4.54%; N, 12.61%; O, 14.40%. Found C, 68.40%; H, 4.50%; N, 12.68%; O, 14.45%.

1-(4-(Tetrazolo[5,1-a]phthalazin-6-yl)phenyl)pyrrolidine-2,5-dione (5)

Sodium azide (10 mmol) was added to a solution of chlorophthalazine **3** (10 mmol) in DMSO (20 mL) and heated under reflux for 6 hours. After cooling, the reaction mixture was poured onto ice. The resulting precipitate was collected by filtration and recrystallized from ethanol, yielding compound **5** as pale yellow crystals. Yield 65%. M.p 216–218°C. IR (KBr, cm⁻¹) : 3052 (CH aromatic), 1779 - 1737 (C=O), 1591 (C=N), and 1410 (N=N). ¹H NMR (DMSO-d₆, 400 MHz, δ, ppm) : 1.02–1.17 (m, 4H, 2CH₂), 7.90–8.07 (m, 8H, aromatic protons). ¹³C NMR (DMSO-d₆, 100 MHz, δ, ppm) : 167.50, 159.60, 137.59, 135.19, 135.04, 133.54, 132.37, 132.01, 129.33, 128.82, 127.89, 127.00, 126.01, 123.90, 29.26. Ms, m/z = 344 (M⁺, 13.95%). Anal. calcd for C₁₈H₁₂N₆O₂ (344.33). C, 62.79%; H, 3.51%; N, 24.41%; O, 9.29%. Found C, 62.85%; H, 3.40%; N, 24.50%; O, 9.15%.

1-(4-(4-((2-Hydroxyethyl)amino)phthalazin-1-yl)phenyl)pyrrolidine-2,5-dione (6)

A solution of chlorophthalazine **3** (10 mmol) in dioxane (40 mL) and ethanolamine (10 mmol) was heated under reflux for 20 hours. After completion, the reaction mixture was concentrated, and the resulting solid was triturated with water, filtered, and recrystallized from ethanol to afforded **6** as pale brown crystals with a 70% yield, M.p 282–284°C. IR (KBr, cm⁻¹) : 3445 (NH), 3332 (OH), 2926 - 2852 (CH aliphatic), 1780 - 1701 (C=O), 1588 (C=N). ¹H NMR (DMSO-d₆, 400 MHz, δ, ppm) : 1.02–1.17 (m, 4H, 2CH₂), 3.40–3.46 (m, 4H, 2CH₂-ethyl), 5.97 (s, 1H, NH, exchangeable), 7.85–8.09 (m, 8H, aromatic protons), 11.58 (s, 1H, OH, exchangeable). ¹³C NMR (DMSO-d₆, 100 MHz, δ, ppm) : 167.50 (CO_{imide}), 163.90 (C-NH), 159.59, 137.59, 135.03, 134.76, 133.53, 132.22, 128.82, 126.99, 126.00, 123.38 (aromatic carbons), 61.48, 58.41, 29.26 (aliphatic carbons). Ms, m/z = 362 (M⁺, 27.16%). Anal. calcd for C₂₀H₁₈N₄O₃ (362.39). C, 66.29%; H, 5.01%; N, 15.46%; O, 13.25%. Found C, 66.20%; H, 4.98%; N, 15.40%; O, 13.20%.

1-(4-(2,3-Dihydroimidazo[2,1-a]phthalazin-6-yl)phenyl)pyrrolidine-2,5-dione (8)

A mixture of compound **6** (10 mmol) and thionyl chloride (2 mL) in anhydrous benzene (30 mL) was heated under reflux for 2 hours, after which the solvent was evaporated under reduced pressure. The resulting solid residue was dissolved in 10% potassium carbonate (20 cm³) and extracted with chloroform. After evaporating the chloroform, free

base **8** was obtained and crystallized from ethanol. Yield 60%. M.p 318 - 320°C. IR (KBr, cm⁻¹) : 3073 (CH aromatic), 1778 - 1682 (C=O), 1574 (C=N). ¹H NMR (DMSO-d₆, 400 MHz, δ, ppm) : 1.05-1.91 (m, 4H, 2CH₂), 2.73-2.88 (m, 4H, 2CH₂), 7.44-7.91 (m, 8H, aromatic protons). Ms, m/z = 344 (M⁺). *Anal.* calcd for C₂₀H₁₆N₄O₂ (344.37) . C, 69.76%; H, 4.68%; N, 16.27%; O, 9.29%; Found C, 69.70%; H, 4.80%; N, 16.27%; and O, 9.35%.

1-(4-(4-Mercaptophthalazin-yl)phenyl)pyrrolidine-2,5-dione (**9**)

A solution of compound **3** (10 mmol) in ethanol (20 mL) was combined with thiourea (10 mmol) and sodium ethoxide (10 mmol) and heated under reflux for 6 hours. After completion of the reaction, the mixture was poured onto ice-water and acidified with acetic acid. The resulting solid was collected by filtration, dried, and recrystallized from ethanol, yielding compound **9** as pale brown crystals with a 60% yield .M.p 212-214°C. IR (KBr, cm⁻¹) : 2553 cm⁻¹ (SH), 1780 - 1702 (CO), 1553 (C=N), 1339 (C=S). ¹H NMR (DMSO-d₆, 500 MHz, δ, ppm): 1.94 (m, 4H, 2CH₂), 7.94-8.26 (m, 8H, aromatic protons), 12.88 (s, 1H, SH exchangeable). ¹³C NMR (DMSO-d₆, 500 MHz, δ, ppm) : 167.08, 159.15, 134.62, 133.11, 131.59, 128.89, 128.38, 128.12, 127.49, 126.56, 125.59, 123.47, 29.51. Ms, m/z = 335 (M⁺, 64.96%), 336 (M+1, 60.55%). *Anal.* calcd for C₁₈H₁₃N₃O₂S (335.38). C, 64.46%; H, 3.91%; N, 12.53%; O, 9.54%; S, 9.56%, found to be C, 64.40%; H, 4.01%; N, 12.50%; O, 9.49%; and S, 9.50%.

(4-(4-(2,5-Dioxopyrrolidin-1-yl)phenyl)phthalazin-1-yl)glycine(**10**)

A mixture of compound **3** (10 mmol) in pyridine (4 mL) containing a few drops of water was combined with glycine (10 mmol) and heated under reflux for 3 hours. Upon completion of the reaction, the mixture was poured onto an ice-HCl solution, leading to the precipitation of a solid. The resulting solid was collected by filtration, thoroughly washed with water, and recrystallized from acetic acid, yielding compound **10** as pale brown crystals with a 75% yield . M.p 211–213°C. IR (KBr, cm⁻¹): 3449 (OH), 3166 (NH), 3004 (CH aromatic), 2924 - 2854 (CH aliphatic), 1708 - 1665 (C=O), 1594 (C=N). ¹H NMR (DMSO-d₆, 400 MHz, δ, ppm) : 2.1 (m, 4H, 2CH₂), 2.88 (s, 2H, CH₂), 4.43 (s, 1H, NH exchangeable), 8.34–8.93 (m, 8H, aromatic protons), 9.46 (s, 1H, OH exchangeable). ¹³C NMR (DMSO-d₆, 500 MHz, δ, ppm) : 167.50 (CO imide), 163.90 (CO), 159.58 (C-NH), 136.77, 135.19, 135.04, 132.38, 132.02, 129.33, 129.27, 128.54, 127.84, 126.07, 125.29, 123.90, 58.41, 29.26. Ms, m/z = 376 (M⁺, 40.72%), 377 (M + 1, 45.32%). *Anal.* calcd for C₂₀H₁₆N₄O₄ (376.37). C, 63.83%; H, 4.29%; N, 14.89%; O, 17.00%; Found C, 63.77%; H, 4.40%; N, 14.50%; O, 16.95%.

1-(4-(3-Oxo-2,3-dihydroimidazo[2,1-a]phthalazin-6-yl)phenyl)pyrrolidine-2,5-dione (**11**)

Acid **8** (10 mmol) was refluxed in acetic anhydride (15 mL) for 3 hours. Upon completion of the reaction, the mixture was cooled and poured onto ice. The resulting solid was filtered, thoroughly washed with water, and recrystallized from ethanol, yielding compound **11** as pale yellow crystals with a yield of 80%. M.p 180–182°C. IR (KBr, cm⁻¹) : 3052 (CH aromatic), 1705 - 1655 (C=O), 1592 (C=N). Ms, m/z = 358 (M⁺). *Anal.* calcd for C₂₀H₁₄N₄O₃ (358.36). C, 67.03%; H, 3.94%; N, 15.63%; O, 13.39%; Found C, 67.10%; H, 3.86%; N, 15.50%; O, 13.5%.

1-(4-(8-Oxo-8H-phthalazino[1,2-b]quinazolin-5-yl)phenyl)pyrrolidine-2,5-dione (**12**)

A mixture of compound **3** (10 mmol) and anthranilic acid (10 mmol) was subjected to fusion in an oil bath at 190–191°C for 2 hours. Upon completion of the reaction, the mixture was cooled and poured into 40 mL of cold water, resulting in the precipitation of a solid product. The obtained solid was collected by filtration and recrystallized from ethanol, yielding compound **12** as pale brown crystals with a yield of 80% .M.p 258–260°C. IR (KBr, cm⁻¹): 3071 (CH aromatic), 1708 - 1699 (C=O), 1576 (C=N). ¹H NMR (DMSO-d₆, 400 MHz, δ, ppm) : 2.16 (m, 4H, 2CH₂), 7.46–8.09 (m, 12H, aromatic protons). Ms, m/z = 421 (M⁺, 26.84%). *Anal.* calcd for C₂₅H₁₆N₄O₃ (421.43). C, 71.42%; H, 3.84%; N, 13.33%; O, 11.42%; Found C, 71.46%; H, 3.89%; N, 13.35%; O, 11.44%.

1-(4-(4-Aminophthalazin-1-yl)phenyl)pyrrolidine-2,5-dione (**13**)

A mixture of chlorophthalazine **3** (10.0 mmol) and ammonium acetate (10.0 mmol) was heated for 2 hours. After cooling, the reaction mixture was triturated with distilled water, followed by filtration and drying. The resulting solid was then recrystallized from ethanol, yielding compound **13** as a solid with a yield of 82% . M.p 221–223°C. IR (KBr, cm⁻¹): 3461 - 3162 (NH₂), 3060 (CH aromatic), 2940 - 2860 (CH aliphatic), 1777 - 1708 (C=O), 1593 (C=N). ¹H NMR (DMSO-d₆, 400 MHz, δ, ppm) : 1.02–1.17 (m, 4H, 2CH₂), 3.74 (s, 2H, NH₂ exchangeable), 7.85–8.08 (m, 8H, aromatic protons). ¹³C NMR spectrum (DMSO-d₆, 100 MHz, δ, ppm) : 167.49 (C=O imide), 159.58 (C-NH₂), along with additional signals corresponding to aromatic carbons (137.57 – 123.89), 31.16 (aliphatic carbons). Ms, m/z = 318 (M⁺, 18.84%). *Anal.* calcd for C₁₈H₁₄N₄O₂ (318.31). C, 67.91%; H, 4.43%; N, 17.60%; O, 10.05%; Found C, 67.88%; H, 4.46%; N, 17.59%; O, 10.10%.

General procedures for synthesis of compounds 14 a-b

A solution of chlorophthalazine **3** (10 mmol) in benzene (40 mL) was combined with o-phenylenediamine and o-aminophenol (10 mmol each) and heated under reflux for 5 hours. After completion of the reaction, the resulting mixture was concentrated through evaporation. The obtained solid product was then recrystallized from ethanol, yielding compounds **14a** and **14b**, respectively.

1-(4-(4-((4-Aminophenyl)amino)phthalazin-1-yl)phenyl)pyrrolidine-2,5-dione (14a)

Yield 70%. M.p 209–211°C. The IR (KBr, cm^{-1}) : 3449 - 3161(NH_2 , NH), 3007 (CH aromatic), 2897 (CH aliphatic), 1780 - 1702 (C=O), 1595 (C=N). ^1H NMR spectrum (DMSO-d_6 , 400 MHz, δ , ppm) : 1.05–1.23 (m, 4H, 2CH_2), 3.37 (s, 2H, NH_2), 7.82 - 8.23 (m, 12H, aromatic protons), 12.82 (s, 1H, NH exchangeable). ^{13}C NMR spectrum (DMSO-d_6 , 500 MHz, δ , ppm) : 167.50 (CO_{imide}), 159.60 (C-NH), 139.35, 137.61, 136.77, 135.18, 135.02, 133.53, 132.36, 131.98, 129.33, 128.80, 128.55, 127.93, 127.87, 126.98, 125.99, 123.42 (aromatic carbons), 29.5 (aliphatic carbon). Ms, m/z = 409 (M^+ , 38.62%). *Anal.* calcd for $\text{C}_{24}\text{H}_{19}\text{N}_5\text{O}_2$ (409.45). C, 70.40%; H, 4.68%; N, 17.10%; O, 7.82%; Found C, 70.50%; H, 4.25%; N, 17.10%; O, 17.75 %.

1-(4-(4-((4-Hydroxyphenyl)amino)phthalazin-1-yl)phenyl)pyrrolidine-2,5-dione (14b)

Yield 68%. M.p 219–221°C. IR (KBr, cm^{-1}) : 3446 - 3102 (NH), (OH), 3051 (CH aromatic), 2924 - 2854 (CH aliphatic), 1737 - 1701 (C=O), 1592 (C=N). ^1H NMR spectrum (DMSO-d_6 , 400 MHz, δ , ppm) : 1.86–2.18 (m, 4H, 2CH_2), 2.87 (s, 1H, NH exchangeable), 7.45–7.99 (m, 12H, aromatic protons), 9.90 (s, 1H, OH exchangeable). Ms, m/z = 410 (M^+ , 25.36%). *Anal.* calcd for $\text{C}_{24}\text{H}_{18}\text{N}_4\text{O}_3$ (410.43). C, 70.23%; H, 4.42%; N, 13.65%; O, 11.69%; Found C, 70.15%; H, 4.49%; N, 13.60%; O, 11.60%.

1-(4-(3-Amino-[1,2,4]triazolo[3,4-a]phthalazin-6-yl)phenyl)-pyrrolidine-2,5-dione (15)

A reaction mixture containing thiosemicarbazide (10 mmol) in absolute ethanol was added to compound **3** and subjected to reflux for six hours. Upon completion of the reaction, the mixture was cooled to room temperature, leading to the precipitation of the product. The obtained solid was filtered, dried, and recrystallized from ethanol to afford compound **15**. Yield 83%. M.p 354–356°C. IR (KBr, cm^{-1}) : 3465 - 3145 (NH_2), 3052 (CH aromatic), 1779 - 1703 (C=O), 1592 (C=N). ^1H NMR (DMSO-d_6 , 500 MHz, δ , ppm) 1.18–1.84 (m, 4H, 2CH_2), 8.56 (s, 2H, NH_2 , exchangeable), 7.22–7.98 (m, 8H, aromatic protons). ^{13}C NMR (DMSO-d_6 , 500 MHz, δ , ppm) 167.10, 159.16, 137.18, 134.77, 134.64, 133.14, 131.59, 128.92, 128.39, 128.14, 127.50, 126.58, 125.61, 123.49, 30.0. Ms, m/z = 358 (M^+ , 60.61%), *Anal.* calcd for $\text{C}_{19}\text{H}_{14}\text{N}_6\text{O}_2$ (358.35). C, 63.68%; H, 3.94%; N, 23.45%; and O, 8.93%. Found C, 63.70%; H, 3.90%; N, 23.50%

Ethyl 2-cyano-2-(4-(4-(2,5-dioxopyrrolidin-1-yl)phenyl)phthalazin-1-yl)acetate (16)

A reaction mixture consisting of compound **3** (10 mmol) and ethyl cyanoacetate in ethanol, along with sodium ethoxide as a base, was subjected to reflux for six hours. Upon completion of the reaction, the resulting mixture was carefully poured into an ice-water solution, leading to the precipitation of the desired product. The solid obtained was subsequently collected through filtration, dried, and purified *via* recrystallization from ethanol, affording compound **16**. Yield 74%. M.p 212–214°C. IR (KBr, cm^{-1}) : 3098 - 3000 (CH aromatic), 2933 - 2894 (CH aliphatic), 2217 ($\text{C}\equiv\text{N}$), 1775, 1709, 1670 ($3\text{C}=\text{O}$), 1587 (C=N). ^1H NMR (DMSO-d_6 , 400 MHz, δ , ppm): 0.08–1.03 (t, 3H, CH_3), 1.20–1.28 (m, 4H, 2CH_2), 4.16–4.28 (q, 2H, CH_2), 4.75 (s, 1H, CH), 7.52–7.94 (m, 8H, aromatic protons). ^{13}C NMR (DMSO-d_6 , 500 MHz, δ , ppm) : 167.01 (CO_{imide}), 163.90 (CO), 159.10, 150.05, 134.70, 134.54, 133.05, 131.54, 128.83, 128.34, 128.05, 127.40, 126.51, 125.52, 123.41, 90.09, 50.59, 29.56, 14.46 (aliphatic carbon). Ms, m/z = 414 (M^+ , 29.68%), *Anal.* calcd for $\text{C}_{23}\text{H}_{18}\text{N}_4\text{O}_4$ (414.42). C, 66.66%; H, 4.38%; N, 13.52%; O, 15.44%. Found C, 66.70%; H, 4.35%; N, 13.50%; O, 15.49%.

1-(4-(4-(3-Amino-5-oxo-4,5-dihydro-1H-pyrazol-4-yl)phthalazin-1-yl)phenyl)pyrrolidine-2,5-dione (17)

A reaction mixture consisting of compound **16** (10 mmol) and hydrazine hydrate (10 mmol) in ethanol (20 mL) was subjected to reflux for six hours. Upon completion of the reaction, the mixture was allowed to cool, leading to the precipitation of the desired product. The obtained solid was collected by filtration, dried, and purified *via* recrystallization from ethanol, yielding compound **18** as a crystalline solid. Yield 71%. M.p 258–260°C. IR (KBr, cm^{-1}) : 3470- 3153 (NH_2), 3100 (NH), 1776, 1708, 1675 ($3\text{C}=\text{O}$), 1593 (C=N). ^1H NMR (DMSO-d_6 , 400 MHz, δ , ppm) : 2.1–2.43 (m, 4H, 2CH_2), 2.88 (s, 2H, NH_2 , exchangeable with D_2O), 3.29 (s, 1H, CH), 7.89–8.07 (m, 8H, aromatic protons), 11.65 (s, 1H, NH, exchangeable with D_2O). Ms, m/z = 400 (M^+ , 13.33%), 401 ($\text{M} + 1$, 9.32%), *Anal.* calcd for $\text{C}_{21}\text{H}_{16}\text{N}_6\text{O}_3$ (400.40). C, 63.00%; H, 4.03%; N, 20.99%; O, 11.99%;. Found C, 64.05%; H, 4.15%; N, 20.80%; O, 12.05%.

5-Amino-4-(4-(4-hydrazinylphenyl)phthalazin-1-yl)-2,4-dihydro-3H-pyrazol-3-one (18)

An equimolar mixture of chlorophthalazine **3** and hydrazine hydrate (10 mmol) was subjected to reflux in ethanol (30

mL) for six hours. Following completion of the reaction, the mixture was allowed to cool, leading to the precipitation of the desired product. The solid was subsequently filtered, dried, and purified through recrystallization from ethanol, yielding pale yellow crystals of compound **18**. Yield 85%. M.p 253–255°C. IR (KBr, cm^{-1}) : 3464 - 3312 (NH_2), 3163 (NH), 1708 (C=O), 1598 (C=N). ^1H NMR (DMSO-d_6 , 400 MHz, δ , ppm) : 2.03 (m, 4H, 2CH_2), 3.40 (s, 2H, NH_2 , exchangeable with D_2O), 6.99–7.55 (m, 8H, aromatic protons), 9.90 (s, 1H, NH , exchangeable with D_2O). ^{13}C NMR (DMSO-d_6 , 100 MHz, δ , ppm) : 167.50, 159.50, 137.59, 135.03, 133.02, 128.83, 127.00, 126.01, 125.60, 123.91, 123.89, 29.26. Ms, m/z = 333 (M^+ , 26.91%), Anal. calcd for $\text{C}_{18}\text{H}_{15}\text{N}_3\text{O}_2$ (333.35). C, 64.86%; H, 4.54%; N, 21.01%; O, 9.60%. Found C, 64.80%; H, 4.60%; N, 20.90%; O, 9.70%.

2.3 Biological assessment

Antimicrobial assay

Experimental

The antibacterial and antifungal properties of the synthesized compounds were assessed through *in vitro* experiments using nutrient agar and Sabouraud dextrose agar, respectively [40]. The antibacterial evaluation targeted *Staphylococcus aureus* (Gram-positive) and *Escherichia coli* (Gram-negative), while the antifungal activity was tested against *Candida albicans* and *Aspergillus niger*. The test solutions were prepared at a concentration of 15 mg/mL, with dimethyl sulfoxide (DMSO) serving as the negative control. For microbial culture preparation, sterilized agar media (20–25 mL per plate) were dispensed into sterile Petri dishes and left to solidify at 25°C. A microbial suspension was prepared in sterile saline and adjusted to match the McFarland 0.5 standard, equivalent to 1.5×10^5 CFU/mL. The turbidity of the suspension was standardized to an optical density (OD) of 0.13 at 625 nm using a spectrophotometer. To ensure uniform microbial distribution, a sterile cotton swab was dipped into the suspension and streaked evenly across the agar surface. After inoculation, the plates were left to dry for 15 minutes. Agar well diffusion was used to evaluate antimicrobial activity, with wells of 6 mm diameter created in the solidified agar using a sterile borer. Each well was filled with 100 μL of the test solution using a micropipette. The plates designated for bacterial testing were incubated at 37°C overnight, while fungal cultures were incubated under appropriate conditions. The experiment was performed in triplicate to ensure accuracy and statistical reliability. Antimicrobial activity was quantified by measuring the diameter of the inhibition zones (mm) around each well.

2.4 Molecular Docking

Computational methods

Structural data for the selected protein receptors were obtained from the RCSB Protein Data Bank (PDB) as summarized in (Table 1). Before molecular docking studies, proteins were preprocessed in PyMOL by removing water molecules, ions, and ligands to optimize docking conditions. Synthesized compounds were designed in BIOVIA Draw, converted to mol2 format via Open Babel [41], and then to pdbqt format using AutoDock Tools for docking readiness. Docking simulations were carried out using AutoDock Vina [42], with compound-specific grid parameters. The resulting protein-ligand interactions were analyzed in Discovery Studio, which provided detailed 2D interaction diagrams, revealing key binding affinities and molecular mechanisms behind the compounds' biological activity.

Table 1. Molecular docking targets of antimicrobial activity, PDB ID's, active site coordinates.

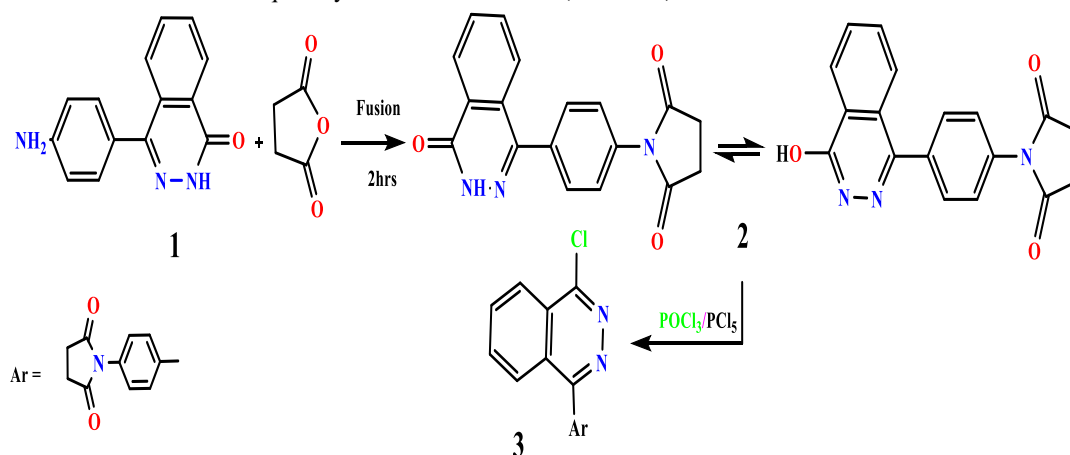
| Organism | | Protein Targets | PD B ID | Active site coordinates: | | | Reference Ligands |
|------------------|-----|--------------------------|------------|-----------------------------|-----------|-----------|----------------------|
| | | | | X | Y | Z | |
| <i>S. aureus</i> | +ve | Dihydropteroate synthase | 1A D4 | 3 6.04 | 4 .35 | 3 6.35 | Ampicillin |
| <i>E. coli</i> | -ve | DNA Gyrase | 7P 2M | - 17.55 | - 4.58 | 1 2.77 | Gentamicin |
| <i>A. niger</i> | | fdc1 of A. niger | 4Z A5 | 1 9.95 | 5 .08 | 2 0.12 | Nystatin |

3. Results and Discussion

3.1 Chemistry

The synthesis of 1-(4-(4-oxo-3,4-dihydrophthalazin-1-yl)phenyl)-pyrrolidine-2,5-dione (**2**), a key starting material, was efficiently achieved with a high yield through the fusion of succinic anhydride with 4-(4-aminophenyl)phthalazin-1(2H)-one (**1**). The precursor compound **1** was synthesized via the reaction of γ -keto acids with hydrazine hydrate in

ethanol, as previously reported [15-16] (*Scheme 1*). The structural elucidation of phthalazine **2** was carried out using various spectroscopic techniques where ^1H NMR spectrum revealed a characteristic singlet at δ 9.92 ppm, corresponding to the NH proton, while another peak at δ 12.88 ppm was attributed to an OH group. Both signals were exchangeable with D_2O , supporting the presence of tautomeric forms. Additional proton resonances between δ 6.98 and 7.56 ppm. The IR spectrum provided further structural confirmation, displaying absorption bands at 3467 cm^{-1} and 3158 cm^{-1} , corresponding to the NH and OH functional groups, respectively. The presence of carbonyl ($\text{C}=\text{O}$) groups was indicated by strong absorption bands at 1780 cm^{-1} and 1700 cm^{-1} , assigned to imidic carbonyls, along with a band at 1595 cm^{-1} , confirming the presence of amidic carbonyl functionalities. Further chemical transformation of phthalazinone (**2**) was successfully achieved through its reaction with phosphorus pentachloride (PCl_5) and phosphorus oxychloride (POCl_3), leading to the formation of 1-(4-(4-chlorophthalazin-1-yl)phenyl)-pyrrolidine-2,5-dione (**3**). This transformation involved the selective chlorination of the phthalazinone core, yielding a highly reactive intermediate that facilitated subsequent synthetic modifications. (*Scheme 1*).



Scheme 1: synthesis of 1-(4-(4-chlorophthalazin-1-yl) phenyl)-1H-pyrrole-2,5-dione (**3**)

Chlorophthalazine (**3**) served as a key reactive intermediate in the synthesis of a novel series of substituted phthalazine and fused phthalazine derivatives. Its remarkable reactivity toward a diverse array of nucleophiles—including carbon-, nitrogen-, oxygen-, and sulfur-based species—enabled the construction of structurally diverse compounds with significant pharmaceutical potential. The mechanistic pathway of compound (**3**) illustrated in (*Figure 2*).

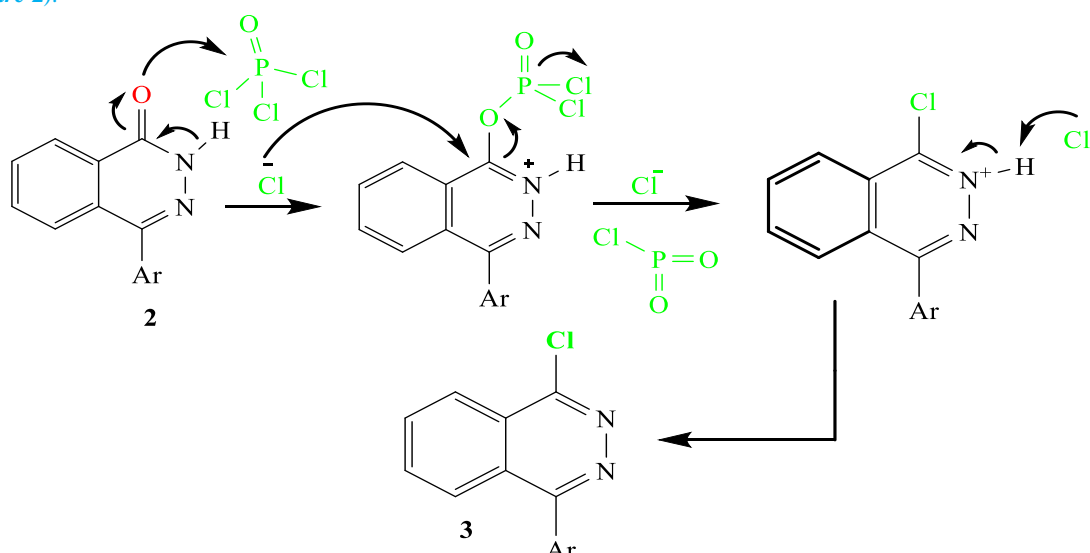


Figure 2. The mechanistic process via which compound **3** is synthesized

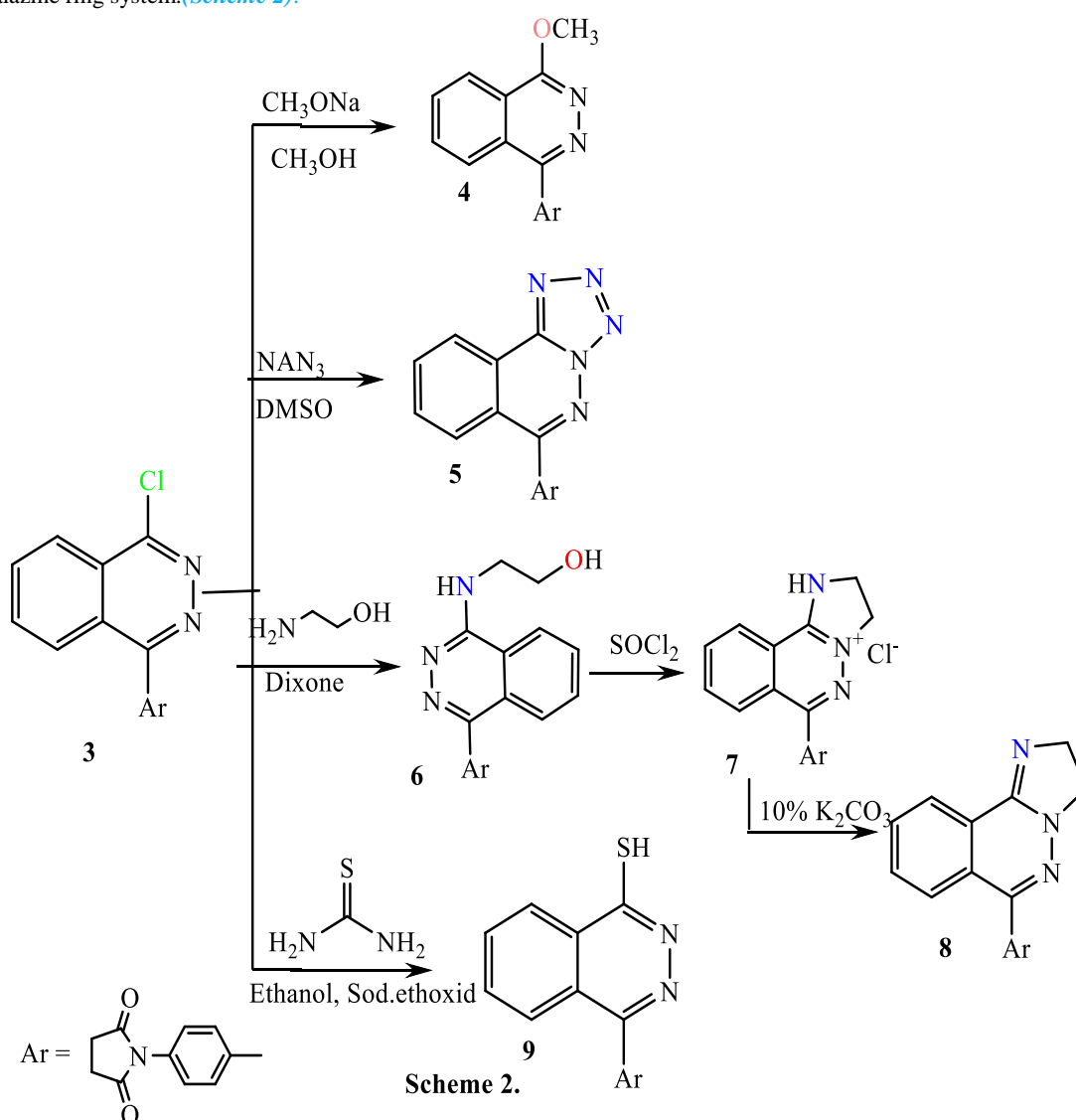
The reaction of chlorophthalazine (**3**) with sodium methoxide in methanol led to the formation of 1-(4-(4-methoxyphthalazin-1-yl)phenyl)pyrrolidine-2,5-dione (**4**). This transformation involved a nucleophilic aromatic

substitution (SN_{NN}Ar) reaction, wherein the highly electrophilic C-4 position of the phthalazine ring was readily substituted by the methoxide anion.

Similarly, when chlorophthalazine (**3**) was treated with sodium azide in dimethyl sulfoxide (DMSO), a cyclization reaction ensued, affording tetrazolo phthalazine (**5**). This reaction proceeded via azide-nucleophilic displacement, followed by intramolecular cyclization, forming a tetrazole-fused system.

The interaction of chlorophthalazine (**3**) with ethanolamine in dioxane led to the formation of compound (**6**), a hydroxyalkylated intermediate. This transformation proceeded via nucleophilic substitution, where the hydroxyl functionality was introduced at the C-4 position of the phthalazine ring. To explore further structural modifications, compound (**6**) was subsequently treated with thionyl chloride (SOCl₂) in benzene, yielding the corresponding phthalazinium chloride (**7**) via chlorination of the hydroxyl group. This cationic phthalazinium was then treated with potassium carbonate (K₂CO₃) in aqueous solution, facilitating the deprotonation and formation of the corresponding free base (**8**).

Additionally, chlorophthalazine (**3**) was subjected to nucleophilic attack by thiourea in the presence of sodium ethoxide, leading to the formation of phthalazine derivative (**9**). This reaction likely proceeded through thiourea-mediated substitution, where the sulfur nucleophile displaced the chlorine atom, forming a thio-substituted phthalazine ring system. (Scheme 2).



The synthesis of phthalazine (**9**) presumably occurred through the mechanism illustrated in (Figure 3)

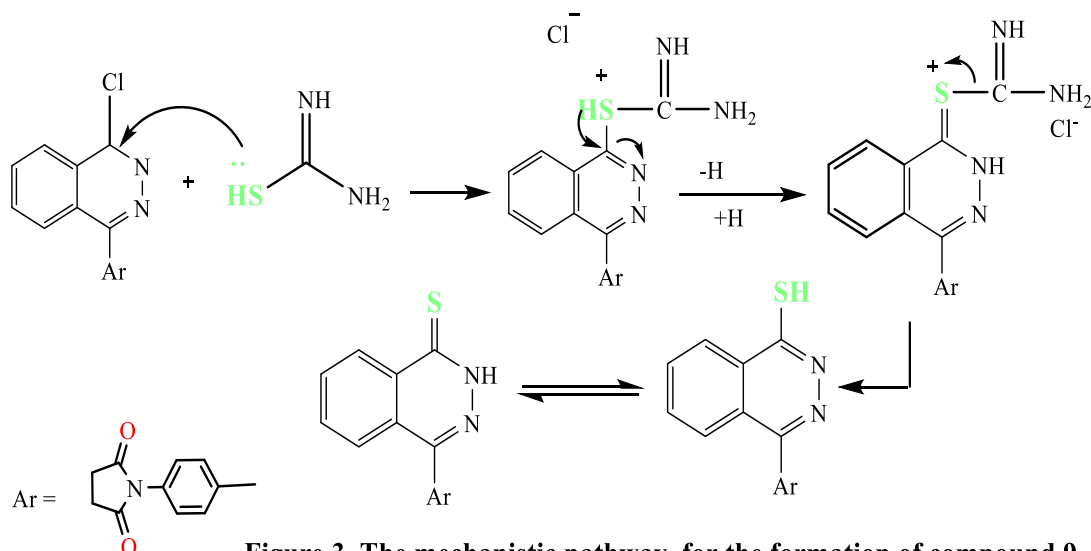


Figure 3. The mechanistic pathway for the formation of compound 9

The chemical reactivity of chlorophthalazine (**3**) with various amino acids was systematically explored, unveiling novel pathways for the synthesis of heterocyclic derivatives. These reactions demonstrated the ability of the phthalazine core to undergo regioselective transformations, leading to structurally diverse bioactive molecules. The reaction of chlorophthalazine (**3**) with glycine in the presence of pyridine and a trace amount of water afforded the amino acid derivative (**10**). This transformation likely proceeded via nucleophilic substitution, where the amino group of glycine displaced the chlorine at C-4 of the phthalazine core. The presence of a carboxyl functional group in the resulting compound (**10**) was confirmed through spectroscopic and elemental analysis, supporting the successful incorporation of the amino acid moiety. To further explore its synthetic potential, compound (**10**) was subjected to cyclization upon treatment with acetic anhydride, yielding the corresponding imidazolidinone derivative (**11**). This intramolecular condensation likely involved the carboxyl and amine functionalities, leading to the formation of a five-membered imidazolidinone ring fused to the phthalazine system.

In contrast, the fusion of chlorophthalazine (**3**) with anthranilic acid in oil bath followed a distinct mechanistic pathway, ultimately yielding a tetracyclic system (**12**). This transformation was rationalized based on the initial formation of an intermediate species (**12'**), in which the carboxyl and amino groups of anthranilic acid engaged in an intramolecular cyclization reaction with the phthalazine core. The final tetracyclic structure (**12**) likely arose via nucleophilic substitution, followed by a spontaneous ring closure, leading to the formation of an extended conjugated system. The presence of fused ring systems in compound (**12**) was validated through spectral characterization and elemental analysis, confirming the expected structural framework (Figure 4).

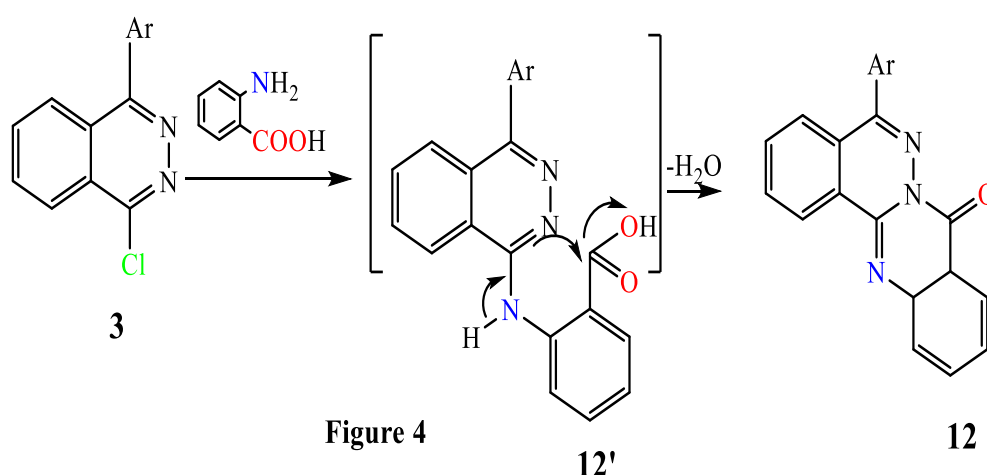
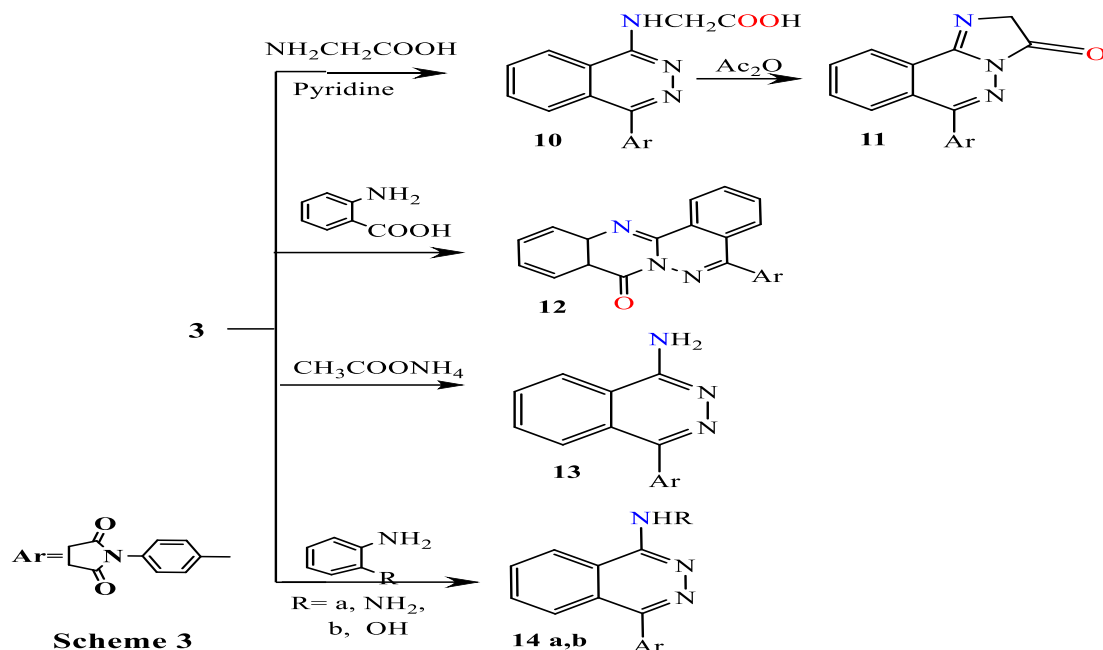


Figure 4

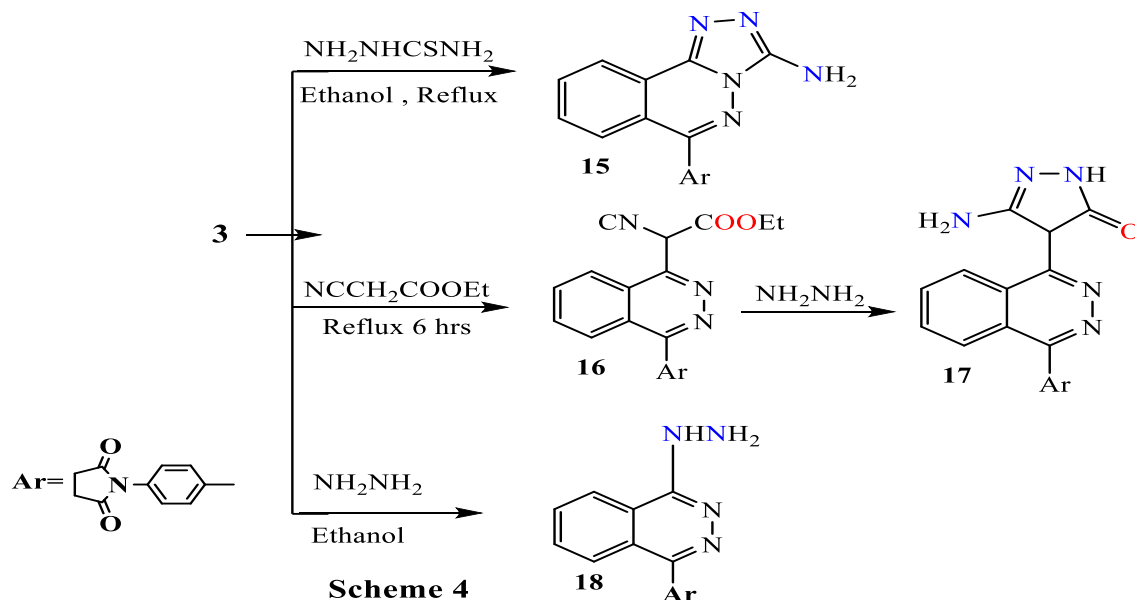
Fusion of chlorophthalazine **3** with ammonium acetate resulted in formation of aminophthalazine **13**.

Whereas, chlorophthalazine **3** underwent reflux with aromatic amines, including O-phenylenediamine and O-aminophenol, in benzene, resulting in the formation of phthalazine derivatives **14a-b**, respectively. (Scheme 3).



However, the reaction of chlorophthalazine **3** with Thiosemicarbazide under reflux in ethanol due to formation of aminotriazolophthalazine **15**.

Furthermore, the reaction of chlorophthalazine **3** with the active methylene compound ethyl cyanoacetate, in the presence of sodium ethoxide as a carbon nucleophile, yielded phthalazine derivatives **16**. The reaction of **16** with hydrazine hydrate in ethanol resulted in the formation of pyrazole derivatives **17**. Furthermore, reactivity of chlorophthalazine **3** towards primary amines like, hydrazine hydrate in *n*-butanol afforded products **18**. (Scheme 4).



3.2 Antimicrobial assay

In vitro, assessment of antibacterial and antifungal activity of synthesized compounds (1-18) against some of pathogenic bacteria and fungi

The newly synthesized phthalazine derivatives (**1–18**) were subjected to in vitro antimicrobial evaluation to assess their antibacterial and antifungal activities against selected pathogenic microorganisms. The assessment was carried out using the agar well diffusion method [40], a widely accepted technique for evaluating the antimicrobial potential of novel compounds. For antibacterial screening, the compounds were tested against *Staphylococcus aureus* (ATCC 13565), representing Gram-positive bacteria, and *Escherichiacoli* (ATCC 10536), representing Gram-negative

bacteria. To ensure a comparative analysis, Ampicillin was used as the standard antibiotic for Gram-positive bacteria, while Gentamicin served as the reference for Gram-negative bacterial strains. The antibacterial activity of each compound was determined by measuring the diameter of the inhibition zone (mm), which provides a direct indication of microbial growth suppression. In addition to bacterial screening, the antifungal efficacy of the synthesized compounds was evaluated against *Candida albicans* (ATCC 10231) and *Aspergillus niger* (ATCC 16404). These fungi were selected due to their clinical relevance in causing opportunistic infections in immunocompromised individuals. The antifungal assay was conducted using Sabouraud dextrose agar (SDA) as the culture medium, ensuring optimal conditions for fungal growth. Nystatin was employed as the standard antifungal agent to provide a reference for evaluating the potency of the synthesized derivatives. To ensure accuracy and reproducibility, all antimicrobial experiments were performed in triplicate, and the inhibition zone diameters were recorded as mean values with standard deviations (\pm SD). These measurements offer a quantitative comparison of the antimicrobial efficacy of the test compounds. The summarized results, including inhibition zone diameters for each microorganism, are presented in Table 2.

Table 2. the antimicrobial results of the examined compounds measured by inhibition zone (mm)

| Microorganism | Gram-positive bacteria | Gram-negative bacteria | Fungi | |
|---------------|--------------------------------------|---|--------------------------------------|---------------------------------------|
| | <i>Escherichia Coli</i> (ATCC:10536) | <i>Staphylococcus Aureus</i> (ATCC:13565) | <i>Candida Albicans</i> (ATCC:10231) | <i>Aspergillus Nigar</i> (ATCC:16404) |
| Compound No. | The inhibition zone (mm) | | | |
| 1 | NA | NA | NA | NA |
| 2 | NA | NA | NA | NA |
| 3 | 14.3 | NA | NA | NA |
| 4 | 13.3 | 12 | NA | NA |
| 5 | 17.7 | NA | NA | NA |
| 6 | 14 | NA | NA | NA |
| 8 | NA | NA | NA | NA |
| 9 | 11 | NA | NA | NA |
| 10 | 11 | NA | NA | NA |
| 11 | NA | NA | NA | NA |
| 12 | NA | NA | NA | NA |
| 13 | NA | NA | NA | NA |
| 14a | 12.3 | 13 | NA | NA |
| 14b | NA | NA | NA | NA |
| 15 | 13 | 14.3 | NA | 13 |
| 16 | 11.3 | NA | NA | NA |
| 17 | 18 | NA | NA | NA |
| 18 | 17.3 | 13 | NA | NA |
| Gentamicin | 27 | | | NA |
| Ampicillin | | 21.3 | | NA |
| Nystatin | | | 21.6 | 19.3 |

NA noactivity

Phthalazine derivatives have long been recognized for their diverse pharmacological applications, particularly their antimicrobial potential. In this study, a series of newly synthesized compounds incorporating the pyrrolidine-2,5-dione moiety were systematically assessed for antibacterial and antifungal activity using the disc diffusion method [40]. The findings, summarized in Table 2, detail the inhibition zone diameters (mm) and activity indices, offering critical insights into their antimicrobial effectiveness. To ensure a comparative evaluation, the antimicrobial activities of the synthesized derivatives were benchmarked against well-established standard antibiotics. Gentamicin and Ampicillin served as reference antibacterial agents, while Nystatin was used to evaluate antifungal potency. Among the tested derivatives, compound 15 exhibited remarkable antibacterial potency, displaying broad-spectrum activity against both *Escherichia coli* and *Staphylococcus aureus*. Interestingly, compound 15 also demonstrated significant antifungal activity against *Aspergillus niger*, even surpassing the efficacy of Nystatin, the standard antifungal agent. The enhanced potency of compound 15 could be attributed to key structural features, such as the presence of electron-donating or withdrawing substituents, which may enhance its ability to interact with microbial targets. Similarly, compounds 4, 14a, and 18 exhibited notable antibacterial activity, particularly against *Escherichia coli* and *Staphylococcus aureus*. Their effectiveness was found to be comparable or superior to Gentamicin and Ampicillin, suggesting their potential as lead compounds for further optimization in antibacterial drug development. In contrast, compounds 3, 5, 6, 9, 10, 16, and 17 displayed moderate antibacterial activity against *Escherichia coli* but did not exhibit significant antifungal effects. The absence of antifungal activity in these derivatives may be attributed to limited fungal cell penetration or insufficient interaction with fungal enzymatic targets. Conversely, compounds 1, 2, 8, 11, 12, 13, and 14b exhibited no detectable antimicrobial activity, indicating that specific functional groups or structural modifications are crucial in governing bioactivity.

3.3 Molecular Docking Study

3.3.1 Docking and interaction with Dihydropteroate synthase of *S. aureus*:

Dihydropteroate synthase serves as a key enzyme in the folate biosynthesis pathway, a crucial metabolic process necessary for bacterial growth and survival. Consequently, targeting this enzyme presents a viable approach for limiting bacterial proliferation. In this study, molecular docking analyses revealed that compounds 4, 14a, 15, and 18 exhibited strong binding affinities to dihydropteroate synthase, with binding energies of -6.90, -6.80, -7.90, and -7.20 kcal/mol, respectively. These binding energies surpass that of the reference antibiotic Ampicillin, which demonstrated a lower binding energy of -6.40 kcal/mol, (as outlined in Table 3, figure 5). The higher binding affinities of these compounds suggest their potential as effective inhibitors of dihydropteroate synthase.

A deeper investigation into the molecular interactions of these compounds revealed their ability to establish hydrogen bonds with key amino acid residues within the enzyme's active site. Specifically, interactions were observed with Arg204, Arg52, Gln105, Lys203, Asp84, Val49, and Asn11, which contribute significantly to ligand stabilization. The presence of these hydrogen bonds strengthens ligand-enzyme binding and enhances inhibitory potential. In addition to hydrogen bonding, the compounds engaged in multiple hydrophobic interactions that further reinforced their binding stability. Alkyl bonding interactions were noted with Lys203, Arg202, and Arg204, while Pi-cation interactions occurred with Arg52 and Arg239. Furthermore, Pi-sulfur interactions were detected with Met128, suggesting a diverse range of molecular interactions that contribute to the overall binding strength of these compounds. Among these interactions, residues such as Arg204, Asp84, and Gln105—located within the catalytic domain of dihydropteroate synthase—played a crucial role in strengthening ligand binding affinity and stability. These key residues are critical for enzyme activity, and their interaction with the tested compounds suggests a strong inhibitory effect that may significantly impair bacterial folate biosynthesis. The findings of this study strongly indicate that these compounds exert their antibacterial effects by targeting and inhibiting dihydropteroate synthase in *Staphylococcus aureus*, thereby disrupting folate biosynthesis and bacterial survival. This proposed inhibitory mechanism aligns with previous research by [38], which utilized molecular docking techniques to analyze small-molecule interactions with *S. aureus* dihydropteroate synthase. The consistency between these findings further supports the potential of these compounds as promising antibacterial agents, warranting further investigation and potential optimization for therapeutic applications.

Table 3: Molecular interactions with the amino acid residues of dihydropteroate synthase from *S. aureus* (PDB ID: 1AD4).

| | Protein | Ligand | Hydrophilic Interactions | Hydrophobic Contacts | | | No. of H-Bonds | No. of Total Bonds | affinity kcal mol-1 |
|---|--|--------|--------------------------|----------------------|----------------------|--------|----------------|--------------------|---------------------|
| | | | Residue (H- Bond) | Length | Residue (Bond type) | Length | | | |
| 1 | Dihydropteroate synthase of <i>S. aureus</i> | 4 | Arg204 (H- Bond) | 2.91 | Arg52, (Pi-cation) | 3.57 | 3 | 6 | -6.90 |
| | | | Arg52 (H- Bond) | 2.61 | Lys203, (Pi-alkyl) | 5.30 | | | |
| | | | Gln105 (H- Bond) | 2.90 | Asn11, (CH-bond) | 3.72 | | | |
| 2 | | 14a | Gln105, (H- Bond) | 1.70 | Arg202, (Pi-alkyl) | 5.01 | 2 | 4 | -6.80 |
| | | | Lys203, (H- Bond) | 2.74 | Arg204, (Pi-alkyl) | 5.49 | | | |
| 3 | | 15 | Arg52 (H- Bond) | 2.74 | Arg52, (Pi-Cation) | 4.66 | 6 | 10 | -7.90 |
| | | | Asp84 (H- Bond) | 2.14 | Arg239, (Pi-cation) | 4.85 | | | |
| | | | | | Arg239, (Pi- cation) | 4.90 | | | |
| | | | | | Met128, (Pi- sulfur) | 2.99 | | | |

| | | | | | | | | |
|---|------------|------------------|------|--------------------|------|---|---|-------|
| 4 | 18 | Val49 (H- Bond) | 2.56 | Lys203, (Pi-alkyl) | 5.38 | 5 | 8 | -7.20 |
| | | Asn11 (H- Bond) | 2.81 | | | | | |
| | | Asp84 (H- Bond) | 2.96 | | | | | |
| | | Arg52 (H- Bond) | 2.60 | | | | | |
| | | Arg204 (H- Bond) | 3.00 | | | | | |
| 5 | Ampicillin | Arg239 (H- Bond) | 2.12 | Pro216, (Pi-alkyl) | 4.30 | 4 | 9 | -6.40 |
| | | Asn11 (H- Bond) | 2.01 | | | | | |
| | | Arg52 (H- Bond) | 2.90 | | | | | |
| | | His241 (H- Bond) | 2.20 | | | | | |
| | | | | | | | | |

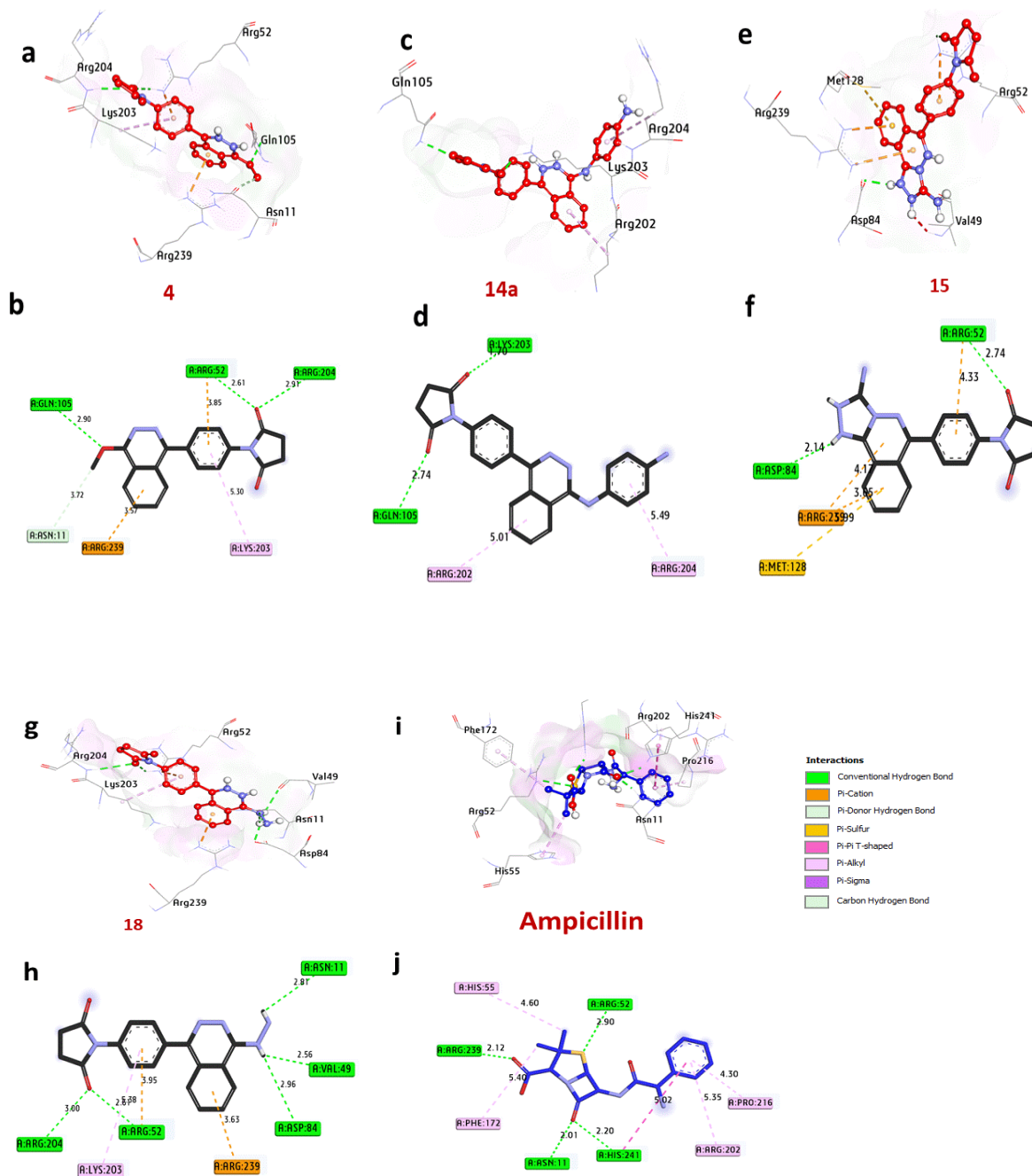


Figure 5. 3D representations of compounds conformations at the binding pocket of dihydropteroate synthase of *S. aureus* (PDB: ID 1AD4): (a and b) **4**, (c and d) **14a**, (e, and f) **15**, (g and h) **18** and (i and j) **Ampicillin**.

3.3.2 Docking and interaction studies with DNA Gyrase of *E.coli* :

To further elucidate the antibacterial potential of the synthesized phthalazine derivatives, molecular docking studies were conducted to assess their interactions with bacterial enzyme targets. As detailed in Table 4 and Figure 6, compounds **4**, **14a**, **15**, and **18** emerged as highly potent bacterial inhibitors, exhibiting superior binding affinities of -7.50, -7.80, -7.30, and -7.40 kcal/mol, respectively. Notably, these values surpass the binding affinity of Gentamicin (-6.10 kcal/mol), a clinically established antibiotic, highlighting their potential as more effective antibacterial agents. A comprehensive interaction analysis revealed that these compounds establish strong hydrogen bonds with key catalytic residues within the active site of the bacterial enzyme, contributing significantly to their inhibitory potential. Specifically, crucial interactions were detected with Asp73, Asn46, Arg76, Gly117, Asp49, Thr165, and Val71, residues known to stabilize the ligand-enzyme complex. These interactions likely play a pivotal role in enhancing the binding strength and specificity of these compounds, thereby increasing their potential to disrupt bacterial enzymatic function. Beyond hydrogen bonding, additional stabilizing interactions were observed, further reinforcing the robust binding of these compounds. Arg76, Thr169, and Asp49 engaged in electrostatic interactions, facilitating strong ligand anchoring within the enzyme's active pocket. Moreover, hydrophobic interactions were also detected, including alkyl bonding with Ala47, Val120, Ile78, Ile94, and Pro79, which contribute to ligand stability. Additionally, C-H bonding with Val43, pi-sigma contacts with Ile78 and Ile94, and pi-cation interactions with Glu50 further enhanced ligand binding, collectively strengthening the overall inhibitory effect. One of the most critical observations of this study was the central role of catalytic site residues in promoting ligand binding. Asp73, Asn46, and Glu50 were identified as essential for ligand stabilization, reinforcing their significance in enzyme inhibition and bacterial growth suppression. These residues are conserved across bacterial species, making them promising targets for the rational design of novel antibiotics. The findings of this molecular docking study align with previous research, including a study by [37], which employed computational docking to investigate inhibitor interactions with DNA gyrase and FabH enzymes, both critical targets in bacterial survival. The consistency of these results with prior studies highlights the predictive power of molecular docking in elucidating structure-activity relationships (SARs) and guiding drug design strategies. The strong binding affinities of compounds **4**, **14a**, **15**, and **18**, along with their ability to interact with key catalytic residues, underscore their potential as lead antibacterial agents. Their capacity to disrupt bacterial enzymatic function, particularly DNA gyrase, suggests that these compounds could serve as promising candidates for further optimization and development in combating bacterial resistance. Future studies focusing on molecular dynamics simulations, ADMET (Absorption, Distribution, Metabolism, Excretion, and Toxicity) profiling, and in vivo efficacy evaluations will be essential to further validate their therapeutic potential.

Table 4: Ligands molecular interactions with amino acids of DNA Gyrase from *E. coli* (PDB ID: 7P2M).

| NO | Protein | Ligand | Hydrophilic Interactions | | Hydrophobic Contacts | | No. of H-Bonds | No. of Total Bonds | affinity kcal mol ⁻¹ |
|----|--|------------|---|----------------------|---|--|----------------|--------------------|---------------------------------|
| | | | Residue (H-Bond) | (H- Length | Residue (Bond type) | Length | | | |
| 1 | DNA Gyrase of <i>E.coli</i> (PDB: ID 7P2M) | 4 | Asp73, (H- Bond) Asn46, (H- Bond) Arg76, (H- Bond) | 1.90 2.69 3.36 | Ala47, (alkyl) Val120, (alkyl) Ile78, (alkyl) Ile78, (pi-sigma) Met95, (pi-sulfur) Val43, (C-H bond) Glu50, (pi-Cation) | 5.48 4.60 5.44 3.51 5.47 3.43 3.82 | 3 | 10 | -7.50 |
| 2 | | 14a | Gly117, (H- Bond) Asn46, (H- Bond) | 2.69 2.14 | Ile78, (alkyl) Ile94, (alkyl) Ile94, (pi-sigma) Ile94, (pi-sigma) | 5.17 5.43 3.90 3.71 | 2 | 6 | -7.80 |
| 3 | | 15 | Asp73, (H- Bond) Asp73, (H- Bond) | 2.10 2.52 | Ile94, (alkyl) Ile78, (alkyl) Ile78, (alkyl) Pro79, (pi-alkyl) Glu50, (pi-Cation) Glu50, (pi-Cation) | 4.95 4.85 4.50 4.84 4.00 3.93 | 2 | 8 | -7.30 |
| 4 | | 18 | Thr165, (H- Bond) Asn46, (H- Bond) Val71, (H- Bond) | 2.19 2.75 2.22 | Ala47, (alkyl) Val120, (alkyl) Val167, (alkyl) Ile78, (Pi-sigma) Met95, (pi-sulfur) Asp73, (pi-Cation) Glu50, (pi-Cation) | 4.92 4.31 5.37 3.54 5.04 3.91 3.66 | 4 | 12 | -7.40 |
| 5 | | Gentamicin | Asp49, (H- Bond) Asn46, (H- Bond) | 2.19 2.34 | Ile94, (alkyl) Ile94, (alkyl) Ile78, (alkyl) | 4.24 5.08 5.05 | 2 | 6 | -6.10 |

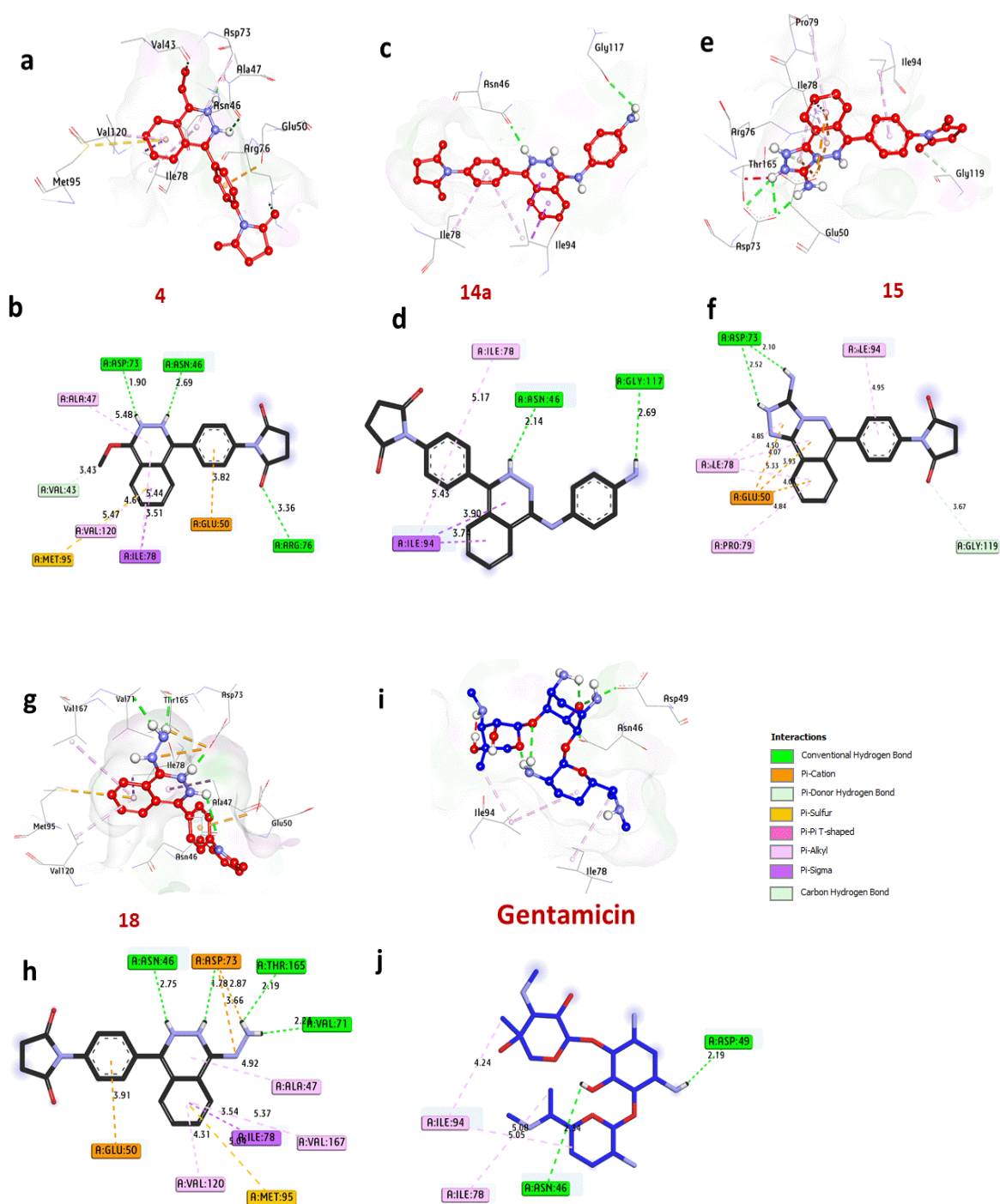


Figure 6: 3D visualizations of compounds within the binding pocket of DNA Gyrase from *E. coli* (PDB ID: 7P2M), displaying (a, b) Compound **4**, (c, d) Compound **14a**, (e, f) Compound **15**, (g, h) Compound **18**, and (i, j) Gentamicin.

3.3.3 Docking and interaction with the *fdc1* of *A. niger* (PDB:ID 43A5):

The development of distinct aromas in fermented beverages, such as wine and beer, is significantly influenced by the enzymatic activity of ferulic acid decarboxylase (FDC1) in *Aspergillus niger*. This enzyme plays a crucial role in breaking down aromatic precursor compounds, thereby shaping the final sensory profile of fermented products. Inhibition of FDC1 has been explored as a potential strategy for modulating aroma profiles and controlling fungal growth in industrial fermentation processes. Molecular docking analyses, as illustrated in [Figure 7](#) and [Table 5](#), revealed that compound **16** exhibited a remarkably high binding affinity of -11.30 kcal/mol, surpassing the binding energy of Nystatin (-10.80 kcal/mol), a well-established antifungal agent. This superior binding affinity suggests that compound **15** may act as an effective inhibitor of fungal FDC1, potentially disrupting its catalytic function. A detailed interaction analysis

demonstrated that the strong binding affinity of compound **15** was primarily facilitated by hydrogen bonding with the catalytic residue Ser224, which contributed to enhanced ligand stability within the enzyme's active site. Additionally, multiple hydrophobic interactions were observed, further reinforcing the ligand's strong binding and inhibitory potential. These included alkyl bonding with Cys316, Ile327, and Ile171, pi-cation interactions with Ser224, pi-sigma bonding with Ile171 and Ile327, pi-sulfur interaction with Met326, and carbon-hydrogen bonding with Ser224. These interactions collectively played a significant role in stabilizing compound **15** within the enzyme's active pocket. Notably, key catalytic residues, including Ser224, Val231, and Ile171, were found to be essential for stabilizing the ligand-enzyme complex. Their involvement in hydrogen bonding and hydrophobic interactions underscores their importance in determining the compound's inhibitory potential. The ability of compound **15** to strongly interact with these residues highlights its potential as an effective antifungal agent targeting FDC1. These findings align with a recent study conducted by [43], which demonstrated the antimicrobial efficacy of compounds targeting *A. niger* FDC1 using molecular docking approaches. The alignment between these studies strengthens the hypothesis that compound **15** could serve as a potent inhibitor of fungal FDC1, presenting valuable prospects for antifungal drug development. Furthermore, the ability of compound **15** to modulate FDC1 activity could have implications in food and beverage fermentation, providing a means to fine-tune aromatic profiles by selectively inhibiting specific fungal enzymatic pathways.

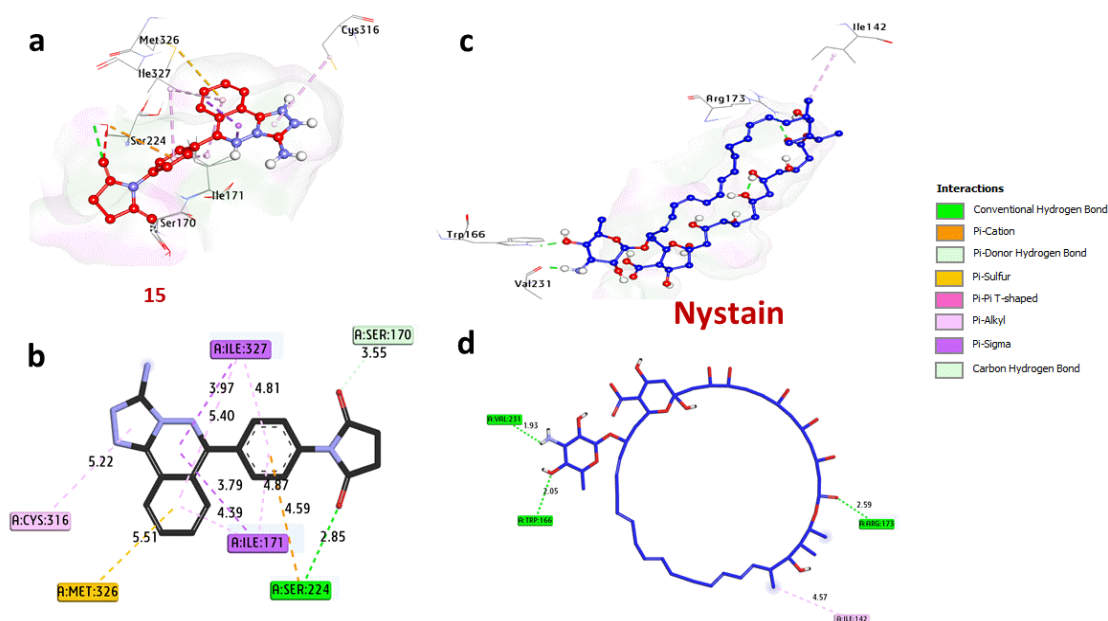


Figure 7: 3D visualizations of compounds within the binding pocket of Fdc1 from *Aspergillus niger* (PDB ID: 4ZA5), showing (a, b) Compound **15** and (c, d) Nystatin.

Table 5: Interactions at the molecular level with the amino acids of fdc1 of *A. niger* (PDB:ID 4ZA5)

| NO | Protein | Compounds | Hydrophilic Interactions | | Hydrophobic Contacts | | No. of H-Bonds | No. of Total Bonds | affinity kcal mol ⁻¹ |
|----|---------------------------------------|-----------|--------------------------|--------|---|--|----------------|--------------------|---------------------------------|
| | | | Residue | Length | Residue (Bond type) | Length | | | |
| 1 | fdcl of <i>A. niger</i> (PDB:ID 5TZ1) | 15 | Ser224, (H- Bond) | 2.85 | Cys316, (Pi-alkyl) Ile327, (Pi-alkyl) Ile171, (Pi-alkyl) Met326, (Pi-sulfur) Ile171, (Pi-sigma) Ile327, (Pi-sigma) Ser224, (Carbon H bond) Ser224, (Pi-cation) | 5.22 4.81 4.81 5.51 3.79 4.81 3.55 4.59 | 1 | 10 | -11.30 |

| | | | | | | | | | |
|---|--|---------|---|----------------------|--------------------|------|---|---|--------|
| 2 | | Nystain | Val231, (H- Bond) Trp166, (H- Bond) Arg173, (H- Bond) | 1.93 2.05 2.59 | Ile142, (Pi-alkyl) | 4.57 | 3 | 4 | -10.80 |
|---|--|---------|---|----------------------|--------------------|------|---|---|--------|

Conclusion

A series of novel phthalazine derivatives incorporating the pyrrolidine-2,5-dione moiety were successfully synthesized with high yields. A variety of elemental and spectral analyses were conducted to verify the structural characterization of these newly developed compounds. Of these compounds **4**, **14a**, **15**, and **18** demonstrated dual antimicrobial properties, underscoring their potential as therapeutic agents. The in vitro evaluations of their pronounced efficacy against both bacterial strains (*E. coli*, *S. aureus*) and fungal species (*A. niger*) indicate a broad-spectrum antimicrobial potential. Molecular docking studies further support these findings by demonstrating significant interactions with key microbial enzymes. Overall, these compounds present promising prospects for the development of multitarget drugs aimed at combating infectious diseases.

Conflicts of Interest

The authors declare that there are no conflicts of interest regarding the publication of this paper.

Acknowledgments

The authors express their gratitude to Benha University, Faculty of Science, and extend their appreciation to the Chemistry Department for their technical support.

References

- [1] N. Dhiman, K. Kaur, and V. Jaitak, *Bioorg. Med. Chem.*, **2020**, 28(15), 115599.
- [2] D. El Sayed, S. M. El Rayes, H. A. Soliman, I. E. AlBalaa, M. S. Alturki, A. H. AlKhzem, M. A. Alsharifd, M. S. Nafie, *RSC Adv.*, **2024**, 14, 13027–13043.
- [3] A.A.H. Abdel-Rahman, S.G. Donia, A. A. F.Wasfy, A. A. Aly, A. Y. El-Gazzar, *Der Pharma Chemica.*, **2013**, 5(1),196-204.
- [4] A. A. Aly, A. A. F. Wasfy, *Indian Journal of Chemistry - Section B Organic and Medicinal Chem.*,**2004**,43(3),629-63.
- [5] A. A. Hassan, R .R. Khattab, A. A. F.Wasfy, K. M. Abuzeid, N. A. Hassan, *J. of Hetero. Chem.*,**2018**, 55(4), 907-912.
- [6]. Ł. Balewski, M. Gdaniec, A. Hering , C. Furman, A. Ghinet, J. Kokoszka, A. Ordyszewska, A. Kornicka, *Int. J. Mol. Sci.*, **2024**, 25, 11495.
- [7] D. Liu, G. Gong, C. Wei, X.Jin,Z.Quan, *Bioorg. Med. Chem. Lett.*, **2016**, 26, (6), 1576-1579.
- [8] I.E. El-Shamy, A.M. Abdel-Mohsen, A.A. Alsheikh, M.M.G. Fouda, S.S. Al-Deyab, M.A. El-Hashash, J. Jancar, *Dyes and Pigments.*, **2015**,113, 357-371.
- [9] I. M. Ghanim., A. A. El Gokha , H. A. A. Abdelaleem., I. E.T. El Sayed , *Egypt. J. Chem.*, 2023, 66(10), 69 - 77.
- [10] B. Holló, J. Magyari, V.Ž. Radovanović, G. Vučković, Z.D. Tomić, I.M. Szilágyi, G. Pokol, K.M. Szécsény, *Polyhedron.*, **2014**, 80, 142-150.
- [11] Y. I. M. Ghanim, A. A. El Gokha , A. H. Abdel Aleem., *Egypt. J. Chem.* 2025, 68(1), 165– 174.
- [12] M. R. Manal., S. Elkhabyr, S. S. Hussein., A. Q. Ghada , Q. Al Anood, *Egypt. J. Chem.*, 2022, 65(13), 331 – 338.
- [13] B.Đ. Glišić, L. Senerovic, P. Comba, H. Wadepohl, A. Veselinovic, D.R. Milivojevic, M.I. Djuran, J.N. Runic, *J. Inorg. Biochem.*, **2016**,155, 115-128.
- [14] M. A. El-hashash, A.Y. Soliman, I. E. EL-Sham, *Turk. J. Chem.*, 2012, 36, 347-366.
- [15] A.F. Wasfy, M.S. Behalo, A.A. Aly, N.M. Sobhi, *Chem. Proc. Eng. Res.*, **2013**, 10, 20-32.
- [16] A.F. Wasfy, M.S. Behalo, A.A. Aly, N.M. Sobhi, *Der Pharma Chemica.*, **2013**, 5, 82-96.
- [17] K.M. Amin, F.F. Barsoum, F.M. Awadallah, N.E. Mohamed, *Eur. J. Med. Chem.*, **2016**, 123, 191-201.

- [18] W.M. Eldehna, S.M. Abou-Seri, A.M. El Kerdawy, R.R. Ayyad, A.M. Hamdy, H.A. Ghabbour, M.M. Ali, D. A. Abou El Ella, *Eur. J. Med. Chem.*, **2016**, 50-62.
- [19] J. Xiang, J. Z. Hong, S. Q. Zhe, *Med Chem Res.*, **2017**, 26, 193546.
- [20] A. A. El-Helby, R. R. Ayyad, H. M. Sakr, A. S. Abdelrahim, K. El-Adl, F. S. Sherbiny, I. H. Eissa, M. M. Khalifa, *J. Mol. Str.*, **2017**, 1130, 333-351.
- [21] I. Graça, E. J. Sousa, P. C. Pinheiro and F. Q. Vieira, *Oncotarget*, **2014**, 5(15), 5950–5964.
- [22] Z. Malinowski, E. Fornal, A. Sumara, R. Kontek, K. Bukowski, B. Pasternak, D. Sroczynski, J. Kusz, M. Małecka and M. Nowak, *Beilstein J. Org. Chem.*, **2021**, 17, 558–568.
- [23] S. Tanaka, M. Tanaka and A. Akashi, *Stroke*, **1989**, 20(12), 1724–1729.
- [24] S. M. Emam, S. M. E. Rayes, I. A. I. Ali, H. A. Soliman, M. S. Nafie, *BMC Chem.*, **2023**, 17(1), 90.
- [25] S. M. El Rayes, G. El Enany, I. A. I. Ali, W. Ibrahim, M. S. Nafie, *ACS Omega*, **2022**, 7(30), 26800–26811.
- [26] S. Elmeligie, A. M. Aboul-Magd, D. S. Lasheen, T. M. Ibrahim, T. M. Abdelghany, S. M. Khojah and K. A. M. Abouzid, *J. Enzyme Inhib. Med. Chem.*, **2019**, 34(1), 1347–1367.
- [27] R. Bolteau, F. Descamps, M. Ettaoussi, D.H. Caignard, P. Delagrangé, P. Melnyk, S. Yous., *Eur. J. Med. Chem.* **2020**, 189, 112078.
- [28] M. Wang, C. Liu, L. Dong, X. Jian, *Chin. Chem. Lett.*, **2007**, 18 (5), 595.
- [29] A. A. Wasfy, *Heteroatom Chemistry*, Volume 14, Issue 7, **2003**, 581-586.
- [30] E. F. Ewies, N. F. El-Sayed, M. El-Hussieny, M. S. Abdel-Aziz, *Egypt. J. Chem.*, **2021**, 64 (12), 7165 – 7173.
- [31] S. K. Kundu, A. Pramanik, A. Patra, *Synlett* 2002(05) (2002) 0823- 0825.
- [32] H.N. Nguyen, V.J. Cee, H.L. Deak, B. Du, K.P. Faber, H. Gunaydin, B.L. Hodous, S.L. Hollis, P.H. Krolikowski, P.R. Olivieri, *The Journal of organic chem.*, **2012**, 77(8), 3887- 3906.
- [33] T.G. Chun, K.S. Kim, S. Lee, T.S. Jeong, H.Y. Lee, Y.H. Kim, W.S. Lee, *Synthetic communications*, **2004**, 34(7), 1301-1308.
- [34] M. Yamaguchi, K. Kamei, T. Koga, M. Akima, T. Kuroki, N. Ohi, *Journal of medicinal Chem.*, **1993**, 36(25) , 4052-4060.
- [35] S. Pathak, K. Debnath, S.T. Hossain, S. K. Mukherjee, A. Pramanik, *Tetrahedron Letters.*, **2013**, 54(24), 3137-3143.
- [36] K. Raval, T. Ganatra, *IP International Journal of Comprehensive and Advanced Pharmacology.*, **2022**, 7(1), 12–16 .
- [37] F. M. Sroor, A.F. El-Sayed, M. Abdelraof., *Archiv Der Pharmazie* **2024**.
- [38] R. E. Khidre, E. Sabry, A.F. El-Sayed, A.A. Sediek, *J. of the Iranian Chemical Society*, **2023**, 20(12), 2923-2947.
- [39] A.H. Jawhari, Y.E. Mukhrish, A. F. El-Sayed, R. E. Khidre, *Current Organic Chem.*, **2023**, 27(10), 860-875.
- [40] A. C. Scott, *Laboratory control of antimicrobial therapy*, Mackie and McCartney: practical medical microbiology, eds Collee J.G., Duguid J.P., Fraser A.G., and Marmion B.P., 13th edn. Churchill Livingstone, Edinburgh, Scotland, **1989**, 2 , 161–181.
- [41] N. M. O'Boyle, M. Banck; C. A. James, C. Morley; T. Vandermeersch; G. R. Hutchison., *J. Cheminform.* **2011**, 3, 33.
- [42] J. Eberhardt; D. Santos-Martins; A. F. Tillack; S. Forli; *J. Chem. Inf. Model.*, **2021**, 61, 8, 3891–3898.
- [43] B. Abd-Elhalim, G. El-Bana, A. El-Sayed, et al. *BMC Biotechnol.*, **2025**, 25, 15.